Lab on a Chip

Cite this: *Lab Chip*, 2011, **11**, 2535

www.rsc.org/loc

PAPER

Lensless imaging for simultaneous microfluidic sperm monitoring and sorting†‡

Xiaohui Zhang,§[a] Imran Khimji,§[a] Umut Atakan Gurkan,[a] Hooman Safaee,[a] Paolo Nicolas Catalano,[a] Hasan Onur Keles,[a] Emre Kayaalp[b] and Utkan Demirci*[ac]

Received 18th March 2011, Accepted 28th April 2011
DOI: 10.1039/c1lc20236g

5.3 million American couples of reproductive age (9%) are affected by infertility, among which male factors account for up to 50% of cases, which necessitates the identification of parameters defining sperm quality, including sperm count and motility. *In vitro* fertilization (IVF) with or without intra cytoplasmic sperm injection (ICSI) has become the most widely used assisted reproductive technology (ART) in modern clinical practice to overcome male infertility challenges. One of the obstacles of IVF and ICSI lies in identifying and isolating the most motile and presumably healthiest sperm from semen samples that have low sperm counts (oligozoospermia) and/or low sperm motility (oligospermaesthenia). Microfluidic systems have shown potential to sort sperm with flow systems. However, the small field of view (FOV) of conventional microscopes commonly used to image sperm motion presents challenges in tracking a large number of sperm cells simultaneously. To address this challenge, we have integrated a lensless charge-coupled device (CCD) with a microfluidic chip to enable wide FOV and automatic recording as the sperm move inside a microfluidic channel. The integrated system enables the sorting and tracking of a population of sperm that have been placed in a microfluidic channel. This channel can be monitored in both horizontal and vertical configuration similar to a swim-up column method used clinically. Sperm motilities can be quantified by tracing the shadow paths for individual sperm. Moreover, as the sperm are sorted by swimming from the inlet towards the outlet of a microfluidic channel, motile sperm that reach the outlet can be extracted from the channel at the end of the process. This technology can lead to methods to evaluate each sperm individually in terms of motility response in a wide field of view, which could prove especially useful, when working with oligozoospermic or oligospermaesthenic samples, in which the most motile sperm need to be isolated from a pool of small number of sperm.

Introduction

According to the American Society for Reproductive Medicine (ASRM), infertility affects about 5.3 million American couples of reproductive age (9%), among which male infertility accounts for 40–50% of cases.[1–3] The leading cause of male infertility is low sperm count, which is usually associated with low sperm motility and impaired sperm function, thus resulting in inability to fertilize an oocyte naturally. Among all available assisted reproductive technologies (ARTs), intra cytoplasmic sperm injection (ICSI) has become a powerful tool to manage male factor infertility. A major challenge to successful ICSI is the selection of highly motile sperm, since sperm quality directly determines whether it will fertilize the oocyte and ultimately result in a viable birth from the fertilized oocyte. Thus, technologies that facilitate the identification and selection of spermatozoa with high motility would increase the ART success rate.

Traditional sperm selection techniques, such as the swim-up method and Percoll gradient centrifugation, have been widely used to separate highly motile sperm from the rest of the sample.[4–6] However, neither of these techniques is optimal: the swim-up method does not provide a high yield of motile spermatozoa;[4] and the centrifugation procedure might have a deleterious effect on sperm.[4] Further, it is challenging to use these

[a]*Bio-Acoustic-MEMS in Medicine (BAMM) Laboratory, Center for Bioengineering, Department of Medicine, Brigham and Women's Hospital, Harvard Medical School, Boston, MA, USA. E-mail: udemirci@rics.bwh.harvard.edu; Fax: +1 617-768-8202; Tel: +1 650-906-9227*
[b]*Jamaica Hospital Medical Center, Department of Obstetrics and Gynecology, Queens, NY, USA*
[c]*Harvard-Massachusetts Institute of Technology Health Sciences and Technology, Cambridge, MA, USA*

† Electronic supplementary information (ESI) available. See DOI: 10.1039/c1lc20236g

‡ Author contributions: U.D. and E.K. developed the idea; U.D., E.K., and I.K. designed the research; X.Z., I.K., H.S., P.N.C., and H.O.K. performed research; X.Z., I.K., U.A.G., and H.S. analyzed data; and X.Z., I.K., E.K. and U.D. wrote the paper.

§ Authors contributed equally.

traditional techniques to isolate highly motile sperm from semen samples complicated by low sperm counts (oligozoospermia),[7] low sperm motility (oligospermaesthenia), or cryopreserved samples of sperm with reduced motility.[8] Since low sperm count or low sperm motility is the most common cause of male infertility, it is likely that the semen samples processed for ICSI procedure will be oligozoospermic, oligospermaesthenic, or both. Therefore, innovative technologies that can be used in the clinical setting to improve the efficiency of motile sperm sorting are needed. These technologies could greatly increase the success rate of IVF for male factor, which in turn would yield a substantial improvement of IVF success overall.

Microfluidics has been widely studied and explored for applications in various areas including biological and chemical analysis,[9–11] point-of-care testing,[12–17] clinical and forensic analysis,[18,19] molecular diagnostics,[20] and medical diagnostics.[15,21] The applications of these technologies to cryobiology[22–24] and reproductive medicine are recent advances.[23,25,26] Microfluidic devices have been used to separate motile sperm with a higher efficiency compared to traditional sperm-sorting methods.[27,28] However, existing approaches require the use of peripheral equipment including pumps and tubing for sperm sorting, which makes them cumbersome to adapt to the clinical settings.

Sperm tracking and motility analyses are usually performed after sorting. Traditionally, optical microscopes have been used to image sperm for computer assisted sperm analysis (CASA) and manual identification of sperm motility for ARTs.[29,30] This classical approach has limitations in tracking a large number of spermatozoa simultaneously due to its small field of view. In addition, the current microscope systems are not compatible with the state-of-the-art in microfluidics, where a minimal image platform is desired to enable compactness, ease-of-use, minimized footprint and portability. Thus, a simple, portable sperm imaging system equipped with a microfluidic-based sperm sorting device could enable real-time sperm motion recording and sorting *in situ*. In addition commercial male fertility test kits for personal home use, such as FertilMARQ[31] or SpermCheck,[32] are now available to assess male fertility or male factor infertility in private. However, these test kits only quantify sperm counts, but cannot quantify sperm motility or the concentration of motile sperms. Such a compact system as the one we developed here would also offer possibilities for disposable, at-home diagnostic testing.

Recently, lensless, on-chip imaging technologies have enabled various applications to overcome some of the limitations related to field of view and healthcare delivery challenges at the point-of-care[13,14,33] by realizing automated, real-time, wide FOV cell monitoring.[17] For instance, Moon *et al.* have shown that a wide FOV lensless CCD image system can improve the efficiency of detecting CD4 cells captured in a microchip.[34] Su *et al.* employed a monochrome holographic lensfree imaging sensor to image a large population of sperm.[35] However, this system only monitors the sperm suspended between a glass slide and cover slip. Hence, it does not have the capability to sort sperm nor to extract the sorted sperm, thus suffering from limited clinical utility. In this study, we integrated a lensless shadow-based CCD imaging system with a microfluidic chip to potentially sort and track sperm *in situ*. With this system, the sperm can be imaged in both horizontal and vertical configurations with additional sorting capability, which is similar to a swim-up column system as is commonly utilized in the clinical setting. We analyzed the sperm samples for velocity, acceleration, and directionality using the recordings of the lensless imaging system captured within the microfluidic channel. This integrated system enables rapid, high-throughput sperm screening to analyze spermatozoa at much higher speed than conventional microscopes through the use of microfluidic devices.

Materials and methods

Sperm preparation

Semen samples were retrieved from B6D2F1 mice aged 7 to 12 weeks from Jackson Laboratories following standard procedures in accordance with institutional guidelines for care and use of animals. Mice were exposed to CO_2 until movement ceased, and euthanized by cervical dislocation. A small incision was made over the midsection, the skin was reflected back, and the peritoneum was entered with sharp dissection to expose the viscera. Both fat pads were pulled down to expose the testes and epididymides. The section of cauda epididymides and vas deferens was excised, and placed into a center-well dish containing 300 μl of Human Tubal Fluid (HTF) (Irvine Scientific, Santa Ana, CA) supplemented with 10 mg ml^{-1} bovine serum albumin (BSA) (Sigma, St Louis, MO). While holding the epididymis in place with a pair of forceps, incisions were made in the distal parts of the epididymis to allow the sperm to flow out. Spermatozoa were pushed out of the vas deferens by stabilizing the organ with an insulin needle and slowly walking a pair of forceps from one end to the other. The dish was then placed in an incubator (37 °C, 5% CO_2) for 10 minutes to allow all sperm to swim out of the epididymis. The epididymides, vas deferens, and larger pieces of debris were then manually extracted and discarded. The sperm suspension was then placed in a 0.5 ml Eppendorf tube, and a thin layer of sterile embryo tested mineral oil (Sigma, St Louis, MO) was added on top to prevent evaporation while allowing for gas transfer. The open tube was then placed in an incubator at 37 °C for 30 min for capacitation. After incubation, a sample of sperm was taken to determine the sperm concentration using the Makler® Counting Chamber (Sefi-Medical Instruments, Haifa, Israel). To pre-sort sperm using the swim-up method, 40 μl of fresh HTF/BSA medium was added on the top of sperm suspension in a 0.5 ml Eppendorf tube subsequent to sperm extraction, followed by placing a thin layer of sterile embryo tested mineral oil on top of the medium. The tube was then placed into an incubator at 37 °C for 1.5 hours to allow for sperm separation.

Microfluidic chip design and fabrication

A combination of polymethylmethacrylate (PMMA) of 1.5 mm thickness (McMaster Carr, Atlanta, GA) and double-sided adhesive (DSA) film of 50 μm thickness (iTapestore, Scotch Plains, NJ) was used to create microfluidic channels (Fig.1A). Both the PMMA and DSA film were cut to 24 mm × 40 mm using a laser cutter (VersaLaser™, Scottsdale, AZ). To create a microchannel, a rectangular section with a width of 4 mm was cut out of the adhesive film using the laser cutter. The DSA film was then placed directly onto the PMMA such that the opposite ends of the rectangular section extended slightly beyond the inlet

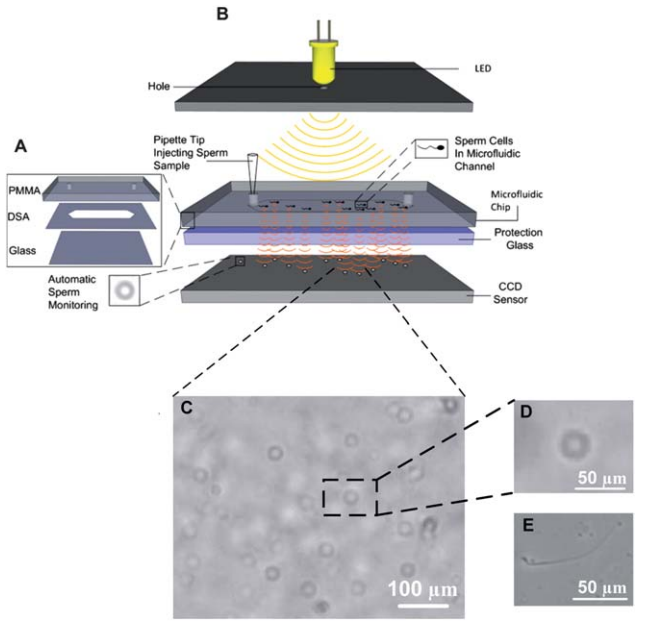

Fig. 1 A schematic illustration of the CCD image platform. (A) The microfluidic chip consists of three layers: PMMA, DSA, and glass coverslip. (B) Lensless CCD image platform integrated with microfluidic chip for sperm tracking. When the light is incident on the microchip, the sperm inside the channel diffract and transmit light. Shadows of the sperm generated by diffraction can be imaged using CCD in one second. (C) Shadow image of the sperm in the microchip channel obtained by the lensless CCD platform. Scale bar is 100 μm. (D) Enlarged single shadow of the sperm from (C). Scale bar is 50 μm. (E) Microscope sperm images taken at 10× objective. Scale bar is 50 μm.

and outlet holes, in effect joining the two. A glass slide was placed onto the other side of the DSA film, such that the height of the channel was determined by and equal to the adhesive layer thickness (Fig. 1A). Inlet and outlet ports were created by cutting holes through the PMMA. The length of the channel is defined as the distance between inlet and outlet.

For sperm imaging, a microchip with a single channel of 3 mm in length, and inlet and outlet port sizes of 0.375 mm was used. To demonstrate the sorting potential of the microfluidic system, the channel length was increased to 7 mm, and inlet and outlet port sizes were increased to 0.65 mm and 2 mm, respectively. The large outlet was particularly designed to extract sperm out of the channel.

Imaging sperm on chip with a lensless CCD system

The microfluidic channel was pre-filled with fresh HTF medium supplemented with 10 mg ml^{-1} BSA. 1 μl of sperm sample was taken from the very top of the swim up column and pipetted into the channel inlet. The microchip was then placed onto a charge-coupled device (CCD) (Imperx, Boca Raton, FL) to obtain shadow patterns of sperm generated by diffraction for analysis (Fig.1B). Fifteen sequenced shadow images for each sperm sample were recorded using a lensless CCD sensor shown in Fig. 1C at a rate of one frame per second. The CCD covered the entire channel, so that all the sperm inside the channel can be recorded. Motile sperm were then identified and tracked using Photoshop (Adobe, San Jose, CA). To image sperm in the vertical configuration, the chip was clamped onto the CCD, and the entire system was rotated 90 degrees. The system was kept in this orientation for the duration of imaging. As a proof of concept of using this lensless CCD system to image sperm inside the chip, we randomly selected 10 sperm cells at each configuration to demonstrate the motility analysis. The sperm from the same male donor mouse were used for imaging in both horizontal and vertical configurations.

Sperm sorting and analysis

The microfluidic channel was first filled with a fresh HTF medium containing 10 mg ml^{-1} BSA. Then the outlet port was filled with 2 μl HTF/BSA medium followed by putting a thin layer of mineral oil on top to avoid medium evaporation. 1 μl of capacitated sperm were removed after capacitation and added to the inlet of the channel, and the microfluidic chip was then placed into an incubator at 37 °C for 30 min. At the end of the incubation, 20 sequenced images were taken for the sperm at both outlet and inlet holes using a microscope (10×) (TE 2000; Nikon, Japan). The sperm count and motility at the microchip inlet and outlet, as well as pre-sorted controls were compared. The sperm under analysis were selected randomly.

Statistical methods

The lensless microfluidic imaging system was evaluated under vertical and horizontal configurations to assess the effect of orientation on the sperm velocity. The sperm cells were imaged with the system in horizontal and vertical configurations and Average Path Velocity (VAP), Straight Line Velocity (VSL), straightness (VSL/VAP) and acceleration were quantified. VAP, VSL and VSL/VAP were statistically analysed for significance of the difference between the groups using a two-sample *t*-test with statistical significance set at 0.05 ($p < 0.05$). To assess the sorting potential of the microfluidic channels utilized, VAP and VSL were further analysed for the non-sorted condition ($n = 33$), inlet ($n = 59$) and outlet ($n = 66$) measurements with One-Way Analysis of Variance (ANOVA) with the Tukey's post-hoc multiple comparison test with statistical significance threshold set at 0.01 ($p < 0.01$). The normality of the data collected was analyzed with Anderson–Darling test.

Results and discussion

In this study, a lensless CCD system was integrated with a microfluidic chip to achieve automatic and wide FOV imaging of a small population of spermatozoa inside a microfluidic channel (Fig. 1B). When using a lensless CCD system for imaging, spermatozoa inside the channel were directly imaged as shadow patterns (Fig. 1C) using uEye (IDS Imaging Development Systems, Inc, Woburn, MA), and spermatozoa movements were tracked. Since the field of view of the CCD sensor (4 mm × 5.3 mm) is approximately 20 times that of a conventional 10× objective lens (1 mm^2), the spermatozoa stay within the CCD view window longer than under a microscope (Fig. 1D and E). Further, larger size CCD systems (37.25 mm × 25.70 mm), which earlier have been shown to reliably detect immobilized cells in microchannels,[17,34] can be used to record sperm over the entire channel and even in multiple channels.

To fertilize eggs *in vivo*, sperm swim towards the eggs against gravity due to the anatomy of female reproductive organ.[36] Clinically, swim-up columns exploit the principle of sperm swimming against the gravitational field for sorting.[4–6] Thus, conducting sperm sorting in a vertical orientation could potentially help us to select more motile sperm than the horizontal orientation. The integrated microfluidic lensless CCD image system presented in this study can be used in a vertical configuration, enabling modalities to record the motility of sperm as they are sorted in real time using the gravitational field as a discriminator. In contrast, it can be challenging to image a vertical chip using a traditional optical microscope, which reflects a significant real-world advantage of integrating lensless microscopy with microfluidics. Sperm motion in both horizontal and vertical microchip configurations was recorded, and the results were displayed in bull's eye plots (Fig. 2). In both configurations, spermatozoa displayed great diversity in their patterns of motion and direction.

To further characterize spermatozoa movements recorded using the lensless imaging system, we tracked the swimming paths and quantified the kinematic parameters that define sperm motility, including average path velocity (VAP), straight line velocity (VSL) and straightness (VSL/VAP) (Fig. 3 and Table S1†). The VAP is referred to as the distance that the sperm covers in the average direction of movement, whereas the VSL is the straight-line distance between the starting and end points of the sperm trajectory. Spermatozoa were tracked in both configurations and their motilities were quantified (Table S1†). Non-motile sperm could also be seen, although only the sperm that showed motility were tracked in this study. Using this portable CCD lensless system, we identified that two sperm cells in the horizontal configuration (H2 and H9 in Table S1†) and two sperm cells in the vertical configuration (V1 and V2 in Table S1†) showed highest motilities, respectively.

The sperm imaged in both (vertical and horizontal) configurations were analyzed statistically for VAP, VSP (Fig. 3A), straightness (Fig. 3B), and acceleration (Fig. 3C). For a small set of mobile capacitated sperm that were monitored for a short period of time, imaging in horizontal and vertical configurations did not result in a statistically significant difference ($p > 0.05$) (Fig. 3). Therefore, the tracking system developed in this study can be used in either configuration. Further, we observed that the accelerations of sperm were within the range of -50 to 30 μm s^{-2} and -75 to 90 μm s^{-2} in horizontal and vertical configurations, respectively. The sperm acceleration spanned a broader range of values at a vertical configuration relative to the horizontal configuration.

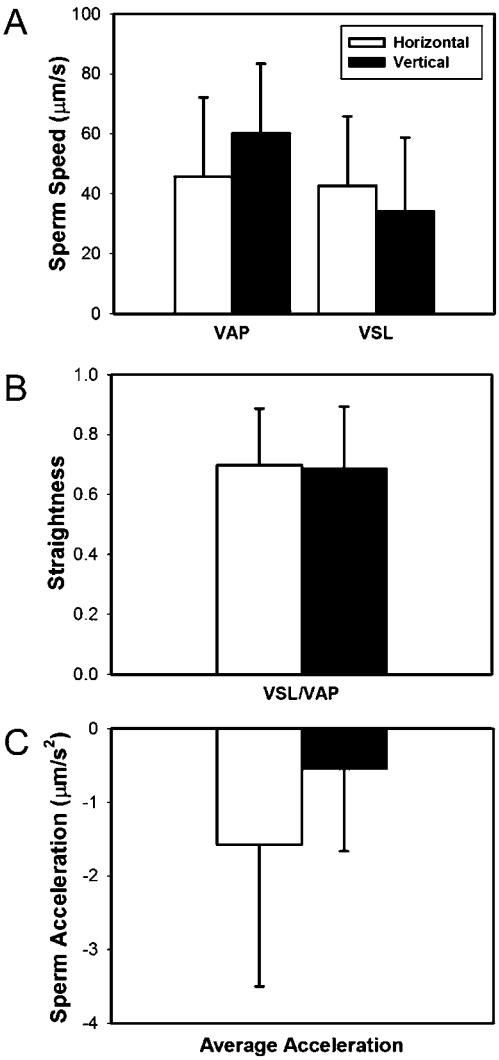

Fig. 3 Comparison of: (A) Average Path Velocity (VAP), Straight Line Velocity (VSL), (B) straightness (VSL/VAP), and (C) average acceleration for sperm cells imaged under horizontal and vertical configurations with a lensless microfluidic system developed in this study ($p > 0.05$).

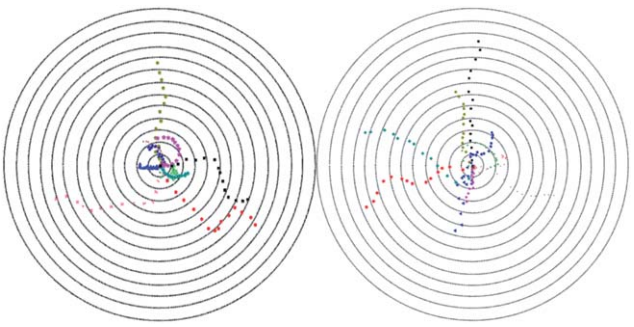

Fig. 2 Bull's eye plot showing sperm motility vectors in the horizontal (left) and vertical (right) configurations. The distance between the adjacent concentric circles is 100 μm.

To demonstrate the capability of the microchip for sperm sorting, sperm motilities at the outlet and inlet were compared to that of non-sorted sperm based on sequenced images obtained using a microscope. As shown in Fig. 4, the motility of sperm at the outlet was significantly higher than those non-sorted sperm and sperm at the inlet post-sorting ($p < 0.01$), indicating that the microfluidic chip can be used to sort the most motile sperm, which can then be collected at the outlet of the microfluidic channel after the sorting process.

In addition, given the wide range of sperm velocities even after sorting, single cell based processing and monitoring has the potential to enable separation of the highest quality motile sperm from the rest utilizing either vertical or horizontal configurations. The sorted sperm can be extracted from the outlet of the

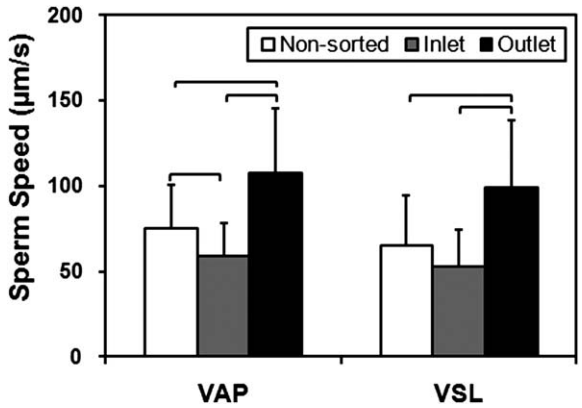

Fig. 4 Comparison of Average Path Velocity (VAP) and Straight Line Velocity (VSL) of sperm for non-sorted condition, and at the inlet and outlet of the 7 mm long microfluidic channel. The VAP and VSL were observed to be significantly greater for the sperm cells imaged at the outlet of the microfluidic channel compared to non-sorted sperm and the sperm at the inlet. Therefore the microfluidic sperm tracking system presented here shows potential to be also used as a sorting platform. (n = 33–66, brackets indicate statistical significance with $p < 0.01$ between the groups).

microfluidic channel either by using a stripper with a fine tip or by pumping medium from the chip inlet. The outlet of the sorting chip was designed to be wide enough (2 mm in diameter) for the tip to easily collect the motile sperm that swam all the way to the outlet. Moreover, the compact and portable microchip-based imaging platform enables sperm analysis to be performed not only in clinical and research settings, but also for at-home testing. Here, we have shown that by integrating microfluidic chip with a lensless imaging system, sperm motion can be recorded *in situ* immediately after sorting inside of the channel, which will be used to quantify the parameters defining sperm motility. To reduce the error when using the lensless CCD imaging system for sperm count, the highest sperm concentration that the system could resolve was estimated using a model equation earlier developed.[17] For a CCD area of 4 mm × 5.3 mm, this model predicted a maximum sperm concentration of 1.6×10^3 sperm per μl. When the sperm is placed in a longer microchannel for sorting, the sperm monitoring needs to be done mostly towards the outlet area, where the motile sperm is. Hence, the microfluidic device can start with sperm concentrations that are as high as that is observed clinically. The most motile sperm sorted at the end of the channel will be within the calculated concentration limits of the shadow based imaging. This is experimentally validated, where we do not see overlapping shadows for post-sorted sperm imaging at the outlet of the microfluidic channel, when 1 μl of sperm sample at 2×10^4 sperm per μl was introduced into the channel from the inlet. The use of a larger area CCD and incorporation of software processing such as video based particle tracking codes can lead to a high degree of scalability, so that millions of spermatozoa may be monitored and analyzed simultaneously.

In summary, we have demonstrated the integrated microfluidic-based lensless CCD imaging system that has the capability to realize wide FOV and automatic recording of sperm inside a channel, where such channels lead to higher motility sperm at the outlets for clinical sorting applications. Such a compact, easy-to-use, and portable system would be useful for fertility clinics to efficiently select most motile sperm for ICSI, especially when working with oligozoospermic or oligospermaesthenic samples. This system can also be beneficial for males, who want to check their fertility at home.

Acknowledgements

Dr Paolo Catalano would like to thank the Fulbright Scholar Program for partially supporting his post-doctoral fellowship in Bio-Acoustic-MEMS in Medicine (BAMM) Laboratory, Center for Bioengineering, Department of Medicine, Brigham and Women's Hospital, Harvard Medical School, Boston, MA, USA. We would like to acknowledge NIH R21 EB007707, and the W.H. Coulter Foundation Young Investigator Award. This was also partially supported by NIH RO1 A1081534, R21 AI087107, and Integration of Medicine and Innovative Technology (CIMIT) under U.S. Army Medical Research Acquisition Activity Cooperative Agreement, and made possible by a research grant that was awarded and administered by the U.S. Army Medical Research & Materiel Command (USAMRMC) and the Telemedicine & Advanced Technology Research Center (TATRC), at Fort Detrick, MD.

References

1 A. Abbey, F. M. Andrews and L. J. Halrnan, *Psychol. Women Q.*, 1991, **15**, 295–316.
2 V. M. Brugh 3rd and L. I. Lipshultz, *Med. Clin. North Am.*, 2004, **88**, 367–385.
3 W. C. Leung and W. E. Rawls, *Virology*, 1977, **81**, 174–176.
4 R. Menkveld, R. J. Swanson, T. J. Kotze and T. F. Kruger, *Andrologia*, 1990, **22**, 152–158.
5 M. Wikland, O. Wik, Y. Steen, K. Qvist, B. Soderlund and P. O. Janson, *Hum. Reprod.*, 1987, **2**, 191–195.
6 J. H. Check, D. Katsoff, J. Kozak and D. Lurie, *Hum. Reprod.*, 1992, **7**, 109–111.
7 S. H. Song, C. W. Bak, J. J. Lim, T. K. Yoon, D. R. Lee and S. W. Kwon, *J. Androl.*, 2010, **31**, 536–539.
8 M. O'Connell, N. McClure and S. E. Lewis, *Hum. Reprod.*, 2002, **17**, 704–709.
9 D. J. Beebe, G. A. Mensing and G. M. Walker, *Annu. Rev. Biomed. Eng.*, 2002, **4**, 261–286.
10 S. C. Jakeway, A. J. de Mello and E. L. Russell, *Fresenius' J. Anal. Chem.*, 2000, **366**, 525–539.
11 T. Chovan and A. Guttman, *Trends Biotechnol.*, 2002, **20**, 116–122.
12 A. J. Tudos, G. J. Besselink and R. B. Schasfoort, *Lab Chip*, 2001, **1**, 83–95.
13 S. Wang, F. Xu and U. Demirci, *Biotechnol. Adv.*, 2010, **28**, 770–781.
14 W. G. Lee, Y. G. Kim, B. G. Chung, U. Demirci and A. Khademhosseini, *Adv. Drug Delivery Rev.*, 2010, **62**, 449–457.
15 M. A. Alyassin, S. Moon, H. O. Keles, F. Manzur, R. L. Lin, E. Haeggstrom, D. R. Kuritzkes and U. Demirci, *Lab Chip*, 2009, **9**, 3364–3369.
16 Y. G. Kim, S. Moon, D. R. Kuritzkes and U. Demirci, *Biosens. Bioelectron.*, 2009, **25**, 253–258.
17 A. Ozcan and U. Demirci, *Lab Chip*, 2008, **8**, 98–106.
18 E. Verpoorte, *Electrophoresis*, 2002, **23**, 677–712.
19 H. Geckil, F. Xu, X. Zhang, S. Moon and U. Demirci, *Nanomedicine (London, U. K.)*, 2010, **5**, 469–484.
20 Y. Huang, E. L. Mather, J. L. Bell and M. Madou, *Anal. Bioanal. Chem.*, 2002, **372**, 49–65.
21 T. Vo-Dinh and B. Cullum, *Fresenius' J. Anal. Chem.*, 2000, **366**, 540–551.
22 Y. S. Song, D. Adler, F. Xu, E. Kayaalp, A. Nureddin, R. M. Anchan, R. L. Maas and U. Demirci, *Proc. Natl. Acad. Sci. U. S. A.*, 2010, **107**, 4596–4600.

23 Y. S. Song, S. Moon, L. Hulli, S. K. Hasan, E. Kayaalp and U. Demirci, *Lab Chip*, 2009, **9**, 1874–1881.
24 U. Demirci and G. Montesano, *Lab Chip*, 2007, **7**, 1428–1433.
25 Y. S. Song, R. L. Lin, G. Montesano, N. G. Durmus, G. Lee, S. S. Yoo, E. Kayaalp, E. Haeggstrom, A. Khademhosseini and U. Demirci, *Anal. Bioanal. Chem.*, 2009, **395**, 185–193.
26 S. Moon, S. K. Hasan, Y. S. Song, F. Xu, H. O. Keles, F. Manzur, S. Mikkilineni, J. W. Hong, J. Nagatomi, E. Haeggstrom, A. Khademhosseini and U. Demirci, *Tissue Eng., Part C*, 2010, **16**, 157–166.
27 B. S. Cho, T. G. Schuster, X. Zhu, D. Chang, G. D. Smith and S. Takayama, *Anal. Chem.*, 2003, **75**, 1671–1675.
28 L. Xie, R. Ma, C. Han, K. Su, Q. Zhang, T. Qiu, L. Wang, G. Huang, J. Qiao, J. Wang and J. Cheng, *Clin. Chem.*, 2010, **56**, 1270–1278.
29 L. Z. Shi, J. M. Nascimento, M. W. Berns and E. L. Botvinick, *J. Biomed. Opt.*, 2006, **11**, 054009.
30 G. Corkidi, B. Taboada, C. D. Wood, A. Guerrero and A. Darszon, *Biochem. Biophys. Res. Commun.*, 2008, **373**, 125–129.
31 *T.B.M.I.T. FertilMARQ™ and* http://www.embryotech.com/consumer/babystart/fmq.htm.
32 *C. SpermCheck Fertility, Inc.*, http://www.contravac.com/products/spermcheck/fertility.php.
33 U. A. Gurkan, S. Moon, H. Geckil, F. Xu, S. Wang, T. J. Lu and U. Demirci, *Biotechnol. J.*, 2011, **6**, 138–149.
34 S. Moon, H. O. Keles, A. Ozcan, A. Khademhosseini, E. Haeggstrom, D. Kuritzkes and U. Demirci, *Biosens. Bioelectron.*, 2009, **24**, 3208–3214.
35 T. W. Su, A. Erlinger, D. Tseng and A. Ozcan, *Anal. Chem.*, 2010, **82**, 8307–8312.
36 *Conceiving the New World Order: the Global Politics of Reproduction*, ed. F. Ginsburg and R. Rapp, University of California Press, 1995.

